

University of Montana

ScholarWorks at University of Montana

Graduate Student Theses, Dissertations, &
Professional Papers


Graduate School

2021

COP9 signalosome component CSN-5 promotes accumulation and function of stem cell regulators FBF-1 and FBF-2

Emily Osterli
University of Montana

Follow this and additional works at: <https://scholarworks.umt.edu/etd>

 Part of the [Cancer Biology Commons](#), [Cell Biology Commons](#), and the [Developmental Biology Commons](#)

Let us know how access to this document benefits you.

Recommended Citation

Osterli, Emily, "COP9 signalosome component CSN-5 promotes accumulation and function of stem cell regulators FBF-1 and FBF-2" (2021). *Graduate Student Theses, Dissertations, & Professional Papers*. 11794.

<https://scholarworks.umt.edu/etd/11794>

This Thesis is brought to you for free and open access by the Graduate School at ScholarWorks at University of Montana. It has been accepted for inclusion in Graduate Student Theses, Dissertations, & Professional Papers by an authorized administrator of ScholarWorks at University of Montana. For more information, please contact scholarworks@mso.umt.edu.

COP9 SIGNALOSOME COMPONENT CSN-5 PROMOTES ACCUMULATION AND
FUNCTION OF STEM CELL REGULATORS FBF-1 AND FBF-2

By

EMILY LIESEL OSTERLI

Associates in Arts and Sciences, Tacoma Community College, Tacoma, WA, 2015
Bachelor of Science in Pharmaceutical Sciences, University of Montana, Missoula, MT,
2020

Doctor of Pharmacy, University of Montana, Missoula, MT, 2021

Thesis

presented in partial fulfillment of the requirements
for the degree of

Master of Science
in Pharmaceutical Sciences and Drug Design

The University of Montana
Missoula, MT

August 2021

Approved by:

Scott Whittenburg, Dean of The Graduate School
Graduate School

Ekaterina Voronina, Chair
Pharmaceutical Sciences and Drug Design
Division of Biological Sciences

Erica Woodahl
Pharmaceutical Sciences and Drug Design
Department of Biomedical and Pharmaceutical Sciences

Kasper Hansen
Pharmaceutical Sciences and Drug Design
Division of Biological Sciences

J. Stephen Lodmell
Cellular, Molecular, and Microbial Biology
Division of Biological Sciences

© COPYRIGHT

by

Emily Liesel Osterli

2021

All Rights Reserved

COP9 signalosome component CSN-5 promotes accumulation and function of stem cell regulators FBF-1 and FBF-2

Chairperson: Ekaterina Voronina

RNA-binding proteins FBF-1 and FBF-2 (FBFs) are required for stem cell maintenance in *C. elegans*, although the mechanisms by which FBFs protein levels are regulated remain unknown. Using a yeast two-hybrid screen, we identified an interaction between both FBFs and CSN-5, a component of the COP9 (constitutive photomorphogenesis 9) signalosome. This highly conserved COP9 complex can affect protein stability through a range of mechanisms including deneddylation, deubiquitination, and phosphorylation (Wolf et al., 2003). Mapping protein-protein interactions between FBFs and CSN-5 suggested that the MPN (Mpr1/Pad1 N-terminal) metalloprotease domain of CSN-5 interacts with the RNA-binding domain of FBFs at physiologically relevant (micromolar) concentrations and this interaction is not RNA-dependent. Furthermore, these conserved domains of the human homologs PUM1 and CSN5 interact as well, thus identifying a protein complex conserved in evolution. We discovered that CSN-5 promotes the accumulation of FBF-1 and FBF-2 proteins in *C. elegans* stem and progenitor cells. Phenotypic analysis results were consistent with *csn-5* contributing to FBF function since *csn-5* germlines are masculinized (produce only sperm similar to *fbf-1/2* loss of function) and show reduced numbers of stem cells. Similar phenotypes were observed in worms mutant for another COP9 holoenzyme component, *csn-6*. Curiously, phenotypes of *csn-2* mutant were clearly distinct, where oocytes were still forming and stem cell numbers were not as affected. Additionally, FBFs protein levels were all reduced in *csn(lf)* mutants, but reduction of FBF-1 was only statistically significant in the *csn(lf)* mutant. This suggests that *csn-5*'s effect on FBFs might be independent of the COP9 holoenzyme. Interestingly, qPCR analysis of *fbf-2* transcript revealed a significant reduction in *csn(lf)* mutants, indicating that we cannot exclude potential transcriptional effects on *fbf* and reduction of FBFs protein levels may partly be a result of a reduction in their transcript levels. Investigating CSN-5 contribution to FBF protein activity and stem cell maintenance will have implications for human stem cell biology and improve our understanding of diseases such as cancer.

Acknowledgements

I would first like to express my sincere gratitude to my mentor, Dr. Ekaterina Voronina. I truly would not be here today without her guidance and support throughout my graduate and undergraduate schooling. I feel very fortunate to have been given the opportunity to work in Katya's lab and gain experiences I would have otherwise missed. Only after joining her lab did I realize that I wanted to pursue a career in research, and I believe having Katya as a mentor played a large role in this decision and in my overall outlook on research. Katya is a strong advocate of active learning and always encouraged me to be a better researcher. Starting early on, she encouraged me to work autonomously and utilize critical thinking when analyzing results, or lack thereof. She is also a big proponent of participating in research conferences and would support my decision to present our work at various meetings. Taken together, Katya has truly helped me grow into a better researcher, and I would not have been able to accomplish what I have without her guidance and support.

As an undergraduate freshman first joining the lab, I definitely required a lot of training and supervision when conducting my initial experiments. I want to convey my thanks to all our past and present lab members who took the time to help me learn the ropes and would happily offer assistance as needed. A special thanks to Dr. Mary Ellenbecker and Dr. Xiaobo (Stacey) Wang, who spent countless hours not only mentoring me throughout my training but would also provide guidance and support over the years. I would also like to thank my fellow lab members for their time and efforts contributing to this project; we wouldn't be where we are today without their assistance.

I would like to sincerely thank my committee advisors Dr. Erica Woodahl, Dr. Kasper Hansen, and Dr. J. Stephen Lodmell for their guidance, advice, and suggestions regarding this project. A special thanks to Erica for her invaluable help coordinating between the pharmacy school and graduate school with this newly established dual degree option and to Kasper for first informing me of this degree path while I was still an undergraduate student.

The faculty and staff at the UM's Skaggs School of Pharmacy, Graduate School, Center for Biomolecular Structure and Dynamics, and Division of Biological Sciences have been incredibly helpful and accommodating as I've progressed through my schooling. I greatly appreciate the efforts of Erika Claxton and Dr. Cherith Smith throughout my time in pharmacy school regarding various paperwork and documentation requirements, scheduling arrangements, and general assistance whenever needed. Surely this Pharm.D./M.S. program would have been exceedingly more difficult without their cooperation and support. I am also thankful for the support of Heidi Boggs, Jill Burke, Cassie Clark, Rochelle Krahn, Sara Jestrab, Ruth Johnson, Karin Schalm, and Kelly Speer over the years.

Without the help of our collaborators and fellow researchers, this project would not have come as far as it has. Specifically, I would like to thank Dr. Steve Sprang, Dr. Baisen (Sam) Zeng, Dr. T.C. Mou, and Cindee Yates-Hansen for their direct contributions to this project, helpful discussions, and sharing various equipment. I would also like to thank Miyuki Hayashi and Dr. Jean-Marc Lanchy for sharing reagents and materials. Additional thanks to the Ryckman lab for allowing us to share some of their

equipment and to Chris Peterson for qPCR training and assistance. Furthermore, I would like to thank Dr. Matthew Sydor for confocal microscopy training and assistance.

My sincere gratitude to my friends and family for their encouragement over the years; I am very fortunate to have their support and to be a part of their lives. Many thanks to Dr. Paul McLean for giving me the opportunity to learn more about the pharmaceutical industry as a summer intern. Additional thanks to my dear friend Kevin Mason, not only because he requested be acknowledged here by name, but also for all his encouragement, time, and efforts helping me over the years.

Lastly, I would like to express my thanks to the good people at Google who invented the Google calendar. Although they now know practically everything I do at all times, I've become entirely too dependent on my Google calendar to quit now and without it my life would have surely collapsed into chaos years ago.

Chapter One - Introduction

Stem cells are the undifferentiated cells that give rise to all other cells which ultimately make up an organism. These nonspecialized cells are capable of both proliferating and self-renewing to produce identical daughter stem cells and differentiating into specialized cells. The ability to both self-renew and differentiate into specialized cells not only provides the body with new cells as it grows, but also replaces specialized cells that may be damaged or lost (Morrison et al., 1997; Chagastelles and Nardi, 2011; Zakrzewski et al., 2019). These characteristics make stem cells an attractive subject of research with promising therapeutic potential. Because stem cells can undergo proliferation and self-renewal as well as differentiate into specialized cells, there has to be a balance between proliferation and differentiation. Without some form of stem cell maintenance, the consequences can be serious. For example, when the balance between proliferation and differentiation is skewed in favor of proliferation and self-renewal, tumors can form (Chagastelles and Nardi, 2011). Conversely, if differentiation into specialized cells is favored over proliferation, the stem cell population cannot be maintained and tissue degeneration can occur (Chagastelles and Nardi, 2011). Most current cancer treatments have taken advantage of this pathophysiology by preferentially targeting proliferating cells or triggering apoptosis in tumor cells (Blagosklonny, 2006; Enane et al., 2018). Alternatively, cancer cells often have poor or arrested differentiation, but may be coaxed into becoming normal cells via differentiation therapy (Yan and Liu, 2016). Since the few differentiation therapies currently in use are limited to subtypes of blood cancers, we need to further investigate the mechanisms balancing proliferation and differentiation to develop more chemotherapies.

Caenorhabditis elegans is a model organism widely used to study stem cell biology. These free-living, transparent nematodes are hermaphrodites and can reach adulthood and produce offspring within a few days (Meneely et al., 2019), making them an attractive organism to utilize in scientific research. *C. elegans* have a single population of stem cells within their germline generating reproductive cells over the animal's lifetime, facilitating the study of their stem cell biology (Kimble and White, 1981; Fig 1). This stem and progenitor cell (SPC) region is located at the distal end of the germline, where cells undergo mitotic divisions. As the cells progress towards the proximal end of the germline, they begin to differentiate and enter meiosis before generating gametes at the proximal end (Hubbard, 2007; Pazdernik and Schedl, 2012; Voronina and Greenstein, 2016). Given the linear progression of cells within the germline, the balance between proliferation and differentiation can be visualized and quantified in this model organism. Since molecular markers of stem cells are readily available, *C. elegans* germline can be stained to reveal the SPC population (Hansen et al., 2004). Another advantage of utilizing *C. elegans* to study stem cell biology is that the consequences of stem cell dysfunction can be seen at the organismal level. Disrupting stem cell regulation can result in many detrimental outcomes, such as abnormal gamete production or tumor formation (Killian and Hubbard, 2005; Hubbard, 2007; Suh et al., 2009). Many genes regulating stem cells in nematodes have homologs in humans, therefore studying stem cell biology in *C. elegans* can advance our understanding of human stem cell biology.

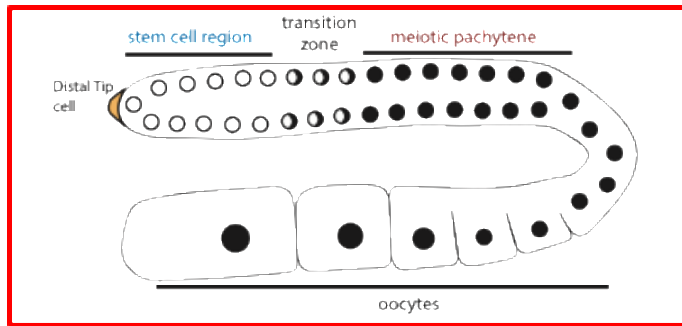
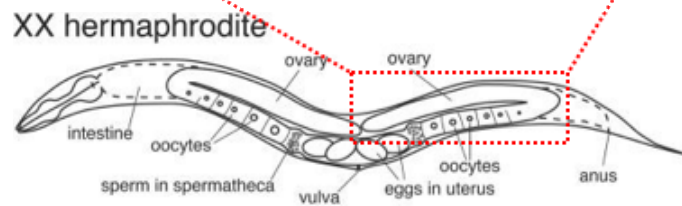


Figure 1.1. Cartoon of *C. elegans* hermaphrodite with a focus on the germline that generates reproductive cells, including oocytes and sperm (Adapted from Ellenbecker et al., 2019 [top], and Zarkower, 2006 [bottom]).



Two important regulators of stem cell maintenance in *C. elegans* are RNA-binding proteins, FBF-1 and FBF-2 (FBFs), that are members of the highly conserved PUF (Pumilio and FBF) family (Wickens et al., 2002). FBFs were initially discovered as repressors of *fem-3*, a gene that encodes a protein facilitating sperm development (Zhang et al., 1997). FBFs promote stem cell maintenance by binding to and repressing target mRNAs that encode developmental regulators which are repressed in stem cells and then activated upon in differentiation and *fbf-1 fbf-2* double mutant gonads lose their germline stem cells (Zhang et al., 1997; Crittenden et al., 2002; Wickens et al., 2002; Wang and Voronina, 2020). Additionally, FBF-1 and FBF-2 facilitate the switch from spermatogenesis to oogenesis as *fbf-1 fbf-2* double mutant gonads fail to undergo oogenesis (Crittenden et al., 2002). FBF target mRNAs relevant to their function in SPC maintenance include the differentiation-promoting protein GLD-1 (Suh et al., 2009). Furthermore, FBFs promote self-renewal of germline stem cells by repressing CKI-2

(Kalchhauser et al., 2011), a cyclin-dependent kinase inhibitor which regulates the decision to enter/exit the cell cycle (Buck et al., 2009). Kalchhauser et al., demonstrate that loss of *cki-2* partially rescues germline stem cell depletion in *fbf-1 fbf-2* double mutants suggesting that FBF-mediated repression of *cki-2* is important for germline stem cell maintenance. In addition to FBF function in supporting stem cell proliferation, FBF-2 has been shown to promote stem cell differentiation and *fbf-2* mutant is predisposed to germline tumors (Wang et al., 2020). Taken together, FBFs clearly have an important role in stem cell maintenance, however, the mechanisms regulating the levels of FBF proteins in stem cells remain unknown.

Human FBF homologs, PUM1 and PUM2 (PUMs), have also been associated with roles in cell cycle regulation, cell fate, and tumor progression (Goldstrohm et al., 2018). By being able to repress target mRNAs like their *C. elegans* counterparts FBF-1 and FBF-2, PUMs can regulate the expression of many genes, including those involved in cancer pathophysiology. Additionally, mouse PUM1 represses the cell cycle inhibitor *cdkn1b*, and therefore promotes cell proliferation (Lin et al., 2019). Human PUM1 has also been shown to help suppress *p27* expression, a negative regulator of the cell cycle, thereby promoting cell proliferation (Kedde et al., 2010). Moreover, hPUM2 has been reported to play a role in promoting chemotherapy resistance and further cancer progression by suppressing apoptosis in non-small cell lung cancer fibroblasts (Wang et al., 2021). Human PUMs are also expressed in embryonic stem cells (Moore et al., 2003; Silva et al., 2020), and their dysregulation has been correlated with the pathophysiology of cancer as PUM expression has been altered in various types of human cancer tissues (Smialek et al., 2021). Specifically, hPUM1 has been found to be overexpressed and

associated with worse prognosis in human cancers such as ovarian, colon, and breast cancers (Guan et al., 2018; Gor et al., 2021; Shi et al., 2021). In mouse models, PUMs have been shown to play a role in the maintenance and proliferation of normal hematopoietic stem cells and PUM dysfunction can promote the onset of acute myeloid leukemia (Spasov and Jurecic, 2003; Naudin et al., 2017). Overall, these data suggest that precise control of PUM activity and protein levels is vital for preventing tumorigenesis.

One of the number of cellular mechanisms regulating protein stability and levels involves the COP9 (constitutive photomorphogenesis 9) signalosome (CSN), a highly conserved enzymatic complex composed of eight subunits, known as CSN1 to CSN8 (Lingaraju et al., 2014). Although initially discovered for its role as a transcriptional repressor (Wei and Deng, 1992), the COP9 signalosome's most studied function is as a regulator of protein degradation (Wei et al., 1994; Chamovitz et al., 1996; Claret et al., 1996; Chamovitz, 2009). COP9 impacts protein degradation by removing a ubiquitin-like protein, NEDD8, from cullin subunits of E3 ubiquitin ligases (Cope et al., 2002; Lingaraju et al., 2014). The overall architecture of CSN resembles the 19S lid of the 26S proteasome, which is responsible for the majority of intracellular protein degradation. CSN subunits 1-4, 7, and 8 contain PCI (proteasome, COP9 signalosome, translation initiation factor) domains similar to the six subunits of the proteasome lid (Lingaraju et al., 2014), and these domains are thought to play a role in regulating protein degradation (Hofmann and Bucher, 1998). COP9 signalosome subunit 5 (CSN5) is the catalytically competent component and contains a Jab1/MPN (Mpr1/Pad1 N-terminal) metalloprotease domain, which is responsible for the complex's deneddylating activity. The signalosome

is inactive without the incorporation of CSN5, and likewise, CSN5 is inactive on its own and unable to neddydate cellular proteins (Cope et al., 2002; Sharon et al., 2009; Echaliier et al., 2013; Lingaraju et al., 2014). Furthermore, CSN5 must dimerize with COP9 subunit CSN6, before the CSN5/CSN6 dimer can be incorporated into the complex and become activated (Birol et al., 2014; Lingaraju et al., 2014). Apart from COP9 subunits, CSN5 has been reported to interact with other cellular proteins, but these interactions have not been extensively studied (Tomoda et al., 2005; Shackleford and Claret, 2010; Yoshida et al., 2013). CSN5 has also been implicated in regulating degradation of several tumor suppressor and oncogene products such as p27, p53, Mdm2, Skp2, and Runx3 (Shackleford and Claret, 2010). Moreover, COP9 subunits CSN5 and CSN6 have been reported to be overexpressed in several human cancers (Figure 1.2; Lee et al., 2011) and Schlierf et al. generated a CSN5 inhibitor that was able to suppress tumor growth of human xenografts in mice (Figure 1.3; Schlierf et al., 2016). Notably, neddylation has also been shown to modulate many biological processes, including tumorigenesis (Zhou et al., 2019). Pevonedistat, a NEDD8-activating enzyme inhibitor, was shown to be clinically efficacious in phase 2 clinical trials for patients with myelodysplastic syndrome, a type of blood cell-related cancer, and acute myeloid leukemia (Sekeris et al., 2021). This NEDD8-activating enzyme inhibitor is currently in phase 3 clinical trials for treatment of the cancer types mentioned above, and more trials are undergoing recruitment for other cancer types as well. Also, a proteasome inhibitor, bortezomib, is currently FDA-approved and first-line treatment for many types of multiple myeloma. However, due to its broad inhibition of proteasome activity, it isn't very specific and results in many undesirable side effects for the patient which can limit

its utility. A drug with greater specificity, such as pevonedistat, may have better utilization in clinical practice if proven safe and efficacious in its ongoing and upcoming clinical trials. Together, these data demonstrate the modulation of the COP9 signalosome/NEDD8/proteasome system has roles in the pathophysiology of some human cancers and targeting more specific components of this system such as CSN5 or the NEDD8-activating enzyme may yield promising cancer therapies.

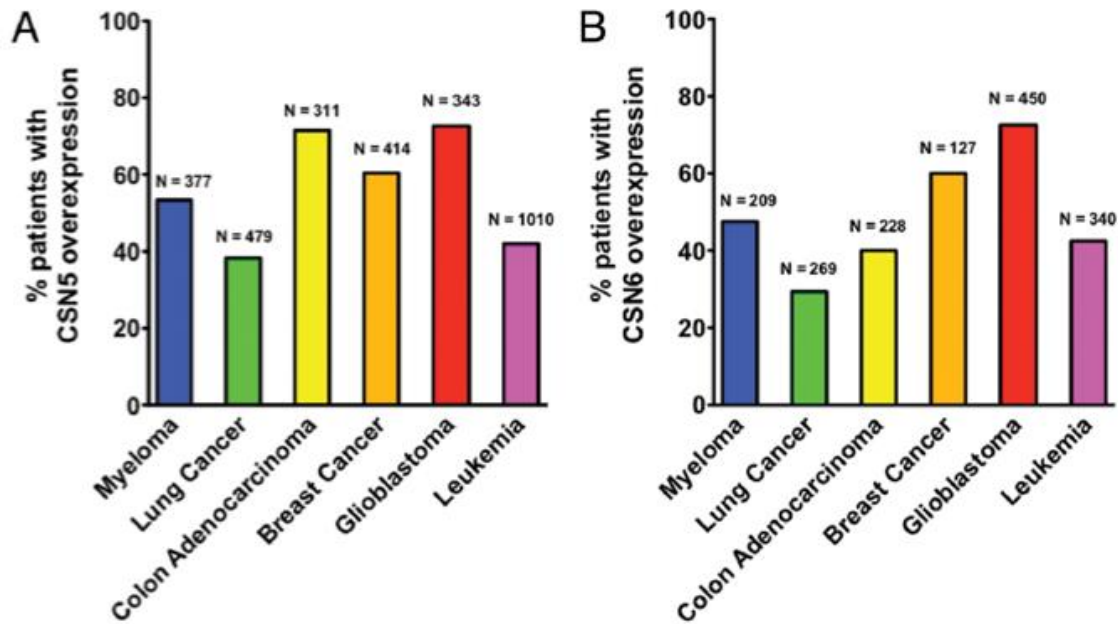


Figure 1.2. Transcriptomic analysis of CSN5 and CSN6 overexpression in human cancer patients (Lee et al., 2011). Patient data sets were obtained from Oncomine and Gene Expression Omnibus. Only patients with more than 40% increase in CSN5 (A) or CSN6 (B) mRNA levels compared to normal tissues were scored as overexpressed.

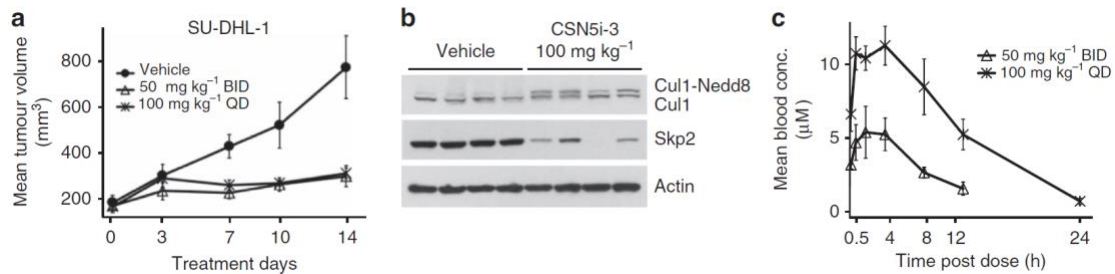


Figure 1.3. CSN5 inhibitor inhibits tumor growth of a human xenograft in mice (Schlierf et al., 2016). (a) Cancer cell line SU-DHL-1 xenografts were grown in mice and were dosed by oral administration with either vehicle control or CSN5 inhibitor. Mean tumor

volumes are shown \pm s.e.m. ($n=4$; $P<0.05$). **(b)** Immunoblotting for neddylation target Cull1 and substrate recognition module Skp2 of tumors excised after treatment completion. **(c)** Pharmacokinetics of CSN5 inhibitor post second to last dose.

In an ongoing yeast-two hybrid screen, our lab identified CSN-5 as a potential binding partner of FBF-2. Given the possibility that this interaction was important for supporting FBF regulatory activity in stem cell maintenance, we have further investigated this interaction and its biological significance in this study.

Chapter Two - Methods and Materials

Nematode strains and culture

All *C. elegans* strains (Table 1) used in this study were cultured on NNGM plates seeded with OP50 as per standard protocols (Brenner, 1974) at 20°C, except for GFP-tagged transgenic strains, which were cultured at 24°C to avoid GFP silencing.

Yeast two hybrid assay

The yeast two hybrid assay was performed by cotransforming the FBF baits and the CSN-5 prey plasmids into yeast PJ69-4a (MATa trp1-901 leu2-3,112 ura3-52 his3-200 gal4Δ gal80Δ LYS2::GAL1-HIS3 GAL2-ADE2 met2::GAL7-lacZ; James et al., 1996). Briefly, the *fbf-2* or *fbf-1* orf were cloned into the MCS of a bait vector pGBKT7 (with TRP selection marker, Clontech, Cat. No. 630491) and the *csn-5* orf was cloned into the MCS of a prey vector pGADT7 (with LEU selection marker, Clontech, Cat. No. 630491). Constructs of the *fbf* baits and the *csn-5* prey were cotransformed into PJ69-4a, and the *fbf* baits and the empty prey pGADT7 were cotransformed as controls. Expression of c-myc tagged FBF-2 or FBF-1 and HA tagged CSN-5 proteins in yeast colonies were confirmed by western blot, using the anti-myc (mouse) 1:1000 and anti-HA (mouse) 1:4000 as primary antibodies, and the Goat anti Mouse HRP 1:2000 as secondary antibody. Serial diluted yeast cultures (at OD600 ~0.2) expressing *fbf* bait and *csn-5* prey (or empty prey) were spotted on the interaction selection plate SD/-Trp, -Leu, -His, -Ade (with 1mM 3-AT to inhibit leaky expression of Histidine reporter) and incubated at 30°C for 4 days. This experiment was repeated for two biological replicates.

GST pulldown assay

Expression constructs containing His₆-FBF-1 and His₆-FBF-2 have been described before (Wang et al., 2016). Truncated FBF expression constructs His₆-FBF-2^{dN1} (amino acids 110-632), His₆-FBF-2^{dN2} (amino acids 164-632), and His₆-FBF-2^{dC1} (amino acids 1-163), His₆-FBF-2^{dN2C2} (amino acids 164-606), His₆-FBF-2^{RBD} (amino acids 164-576), and His₆-FBF-1^{RBD} (amino acids 161-573) were generated by PCR from full-length FBF-2 or FBF-1 and inserted into pETDuet-1 plasmid (EMD Millipore). Full-length *C. elegans* CSN-5 (amino acids 1-368) was amplified from N2 Bristol cDNA and cloned into pGEX-KG plasmid. Truncation constructs CSN-5^N (amino acids 1-258) and CSN-5^C (amino acids 259-368) constructs were made by PCR from full-length CSN-5 and inserted into pGEX-KG plasmid. Human homolog CSN5^N (amino acids 1-257) was amplified from HEK293 cDNA and cloned into pGEX-KG plasmid. Human homolog PUM1^{HD} (isoform 1, amino acids 828-1176) was amplified from HEK293 cDNA and cloned into pETDuet-1 plasmid (EMD Millipore). Mutagenesis of the reported FBF-2 binding motif, 231KxxL234, on CSN-5 was performed using a Q5 Site-Directed Mutagenesis Kit (New England BioLabs, Cat. No. E0552S). All constructs were sequenced and transformed into *Escherichia coli* strain BL21(DE3) for expression. Expression of His-tagged FBF protein constructs were induced with 0.1 mM IPTG at 15°C for 20-24 hours. Expression of GST alone or GST-tagged CSN-5 protein constructs were induced with 0.1 mM IPTG at 37°C for 4.5 hours. Pellets of induced bacteria were collected and resuspended in lysis buffer (20 mM Tris pH 7.5, 250 mM NaCl, 10% glycerol, 1 mM MgCl₂, 0.1% Triton X-100) containing 10mM beta-mercaptoethanol (BME), 1 mM PMSF, protease inhibitor cocktail (1 tablet per 50 mL; Roche, Cat. No. 05892953001), 0.5 mg/ml lysozyme, and 6 µg/ml DNase I,

rotated at 4°C for 1 hour to lyse, and cleared by centrifugation at 1110 g for 20 min. Cell lysate of GST alone or GST-tagged CSN-5 constructs were bound to glutathione beads in 20 mM Tris pH 7.5, 250 mM NaCl, 10% glycerol, 0.1% Triton X-100, 10 mM BME, 1 mM PMSF, and protease inhibitor cocktail (1 tablet per 50 mL; Roche, Cat. No. 05892953001) for 1 hour at 15°C. Binding reactions with 6xHis-tagged preys were incubated at 15°C for 3 hours and washed four times with 10 mM Tris pH 7.5, 150 mM NaCl, 0.1% NP-40, and 0.5 mg/ml BSA. For elution, beads were heated to 95°C for 5 minutes in sodium dodecyl sulfate (SDS) sample buffer and 10 mM dithiothreitol (DTT). Protein samples from pulldown assays were separated using Mini-PROTEAN TGX 4-20% precast gels (Bio-Rad, Cat. No. 4561093) and visualized using either Coomassie (GST alone and GST-tagged constructs) or by Western blotting (His₆-FBF constructs). Monoclonal anti-polyHistidine (mouse IgG2a isotype) primary antibody (1:2000; Sigma-Aldrich, Cat. No. H1029) and peroxidase—conjugated goat anti-mouse IgG2a specific secondary antibody (1:1000; SouthernBiotech, Cat. No. 1080-05) was used to visualize His₆-FBF protein constructs and anti-GST rabbit IgG primary antibody (1:6000; Sigma-Aldrich, Cat. No. G7781) and peroxidase-conjugated goat anti-rabbit IgG secondary antibody (1:5000; Jackson ImmunoResearch, Cat. No. 111-035-003) was used to visualize GST and GST-tagged CSN-5 constructs.

Western blot analysis

Western blot analysis of FBF levels in *csn(lf)* mutants was carried out in 3 biological replicates. 50 worms were individually picked from synchronous cultures [*V5::fbf-2*, *V5::fbf-2; csn-5(ok1064)*, *V5::fbf-2; csn-6(ok1604)*, or *csn-2(ok1288); V5::fbf-2*],

deposited in 1.75% SDS-PAGE sample buffer with 75mM DTT, and boiled for 15 minutes prior to SDS-PAGE gel electrophoresis. Proteins from worm lysate (50 worms per lane) were separated on a 7.5% gel and transferred to a 0.2 μ m PVDF membrane (EMD Millipore, Cat. No. ISEQ00010). After transfer, membranes were blocked in TBS/0.05% Tween 20/5% milk powder and the blots probed with monoclonal mouse anti- α -tubulin (1:500; Sigma-Aldrich, Cat. No. T6199), monoclonal mouse IgG2a anti-V5 (1:500; Invitrogen, Cat. No. R96025), and polyclonal rabbit anti-FBF-1 (1:10; Voronina et al., 2012; PA2388) primary antibodies diluted in blocking solution. Peroxidase-conjugated goat anti-mouse IgG (1:5000; Jackson ImmunoResearch, Cat. No. 115-035-174) and peroxidase-conjugated goat anti-rabbit (1:5000; Jackson ImmunoResearch, Cat. No. 111-035-003) secondary antibodies were used. Membranes were developed using Luminata Crescendo Western HRP substrate (EMD Millipore, Cat. No. WBLUR0500 or WBLUCC0500) and visualized using Bio-Rad ChemiDoc MP Imaging System. Band intensities were quantified using Image Lab software version 5.1.

Immunofluorescence

Adult hermaphrodites were washed in M9 and germlines were dissected on poly-L-lysine treated slides, covered with a coverslip to ensure attachment to slide surface, and flash frozen on aluminum blocks chilled on dry ice for 30 minutes. The samples were fixed for 1 minute in 100% methanol (-20°C) followed by 5 minutes in 2% paraformaldehyde/100 mM K₂HPO₄ (pH 6) at room temperature. The samples were then blocked in PBS/0.1% BSA/0.1% Tween-20 (PBS-T/BSA) for 30 minutes at room temperature. Next, samples were incubated with primary antibody diluted in PBS-T/BSA

overnight at 4°C. Samples were then washed with PBS-T/BSA three times for 10 minutes each wash, before incubating with secondary antibody diluted in PBS-T/BSA for 2 hours at room temperature in a light-sealed humid chamber. Samples were washed again three times for 10 minutes each wash before adding 10 µL Vectashield with DAPI (Vector Laboratories, Cat. No. H-1200) and cover-slipping. Primary antibodies were rabbit anti-REC-8 (1:500; Novus Biologicals, Littleton, CO, Cat. No. 29470002), monoclonal mouse IgG2a anti-V5 (1:500; Invitrogen, Cat. No. R96025), and polyclonal rabbit anti-FBF-1 (1:10; Voronina et al., 2012; PA2388). Secondary antibodies were Alexa Fluor 488-conjugated goat anti-rabbit IgG (1:200; Jackson ImmunoResearch, Cat. No. 111-545-144), and Alexa Fluor 594-conjugated goat anti-mouse IgG (1:500; Jackson ImmunoResearch, Cat. No.115-585-146). Images were acquired with a Leica DFC300G camera attached to a Leica DM5500B microscope with a 40x LP FLUOTAR NA1.3 objective using LAS-X software (Leica) and stitched together using Adobe Photoshop CS3.

Phenotypic analysis

C. elegans were synchronized by bleaching and hatched L1 larvae were plated on NNGM plates with OP50 bacteria, grown at 20°C, and harvested after 72 hours. Gonads were dissected and stained for DNA with DAPI and were scored for % with abnormal oocytes (defined by <3 oocytes per germline, sick or not condensed, increased chromosomes, and/or endomitotic oocytes), % masculinization of germline (Mog), and % without gametes.

Germline SPC zone measurement

C. elegans were synchronized by bleaching and hatched L1 larvae were plated on NNGM plates with OP50 bacteria, grown at 20°C, and harvested after 72 hours. Gonads were dissected and stained for mitotic marker REC-8 (Hansen et al., 2004), and the number of stem and progenitor cells was measured by counting the total number of cells positive for REC-8 staining using Cell Counter plug-in in Fiji (Schindelin et al., 2012).

RNA extraction and RT-qPCR

C. elegans were synchronized by bleaching and hatched L1 larvae were plated on NNGM plates with OP50 bacteria, grown at 20°C, and collected after 72 hours. 200 worms were collected per biological replicate and stored in Trizol (Invitrogen, Cat. No. 15596026) at -80°C. The qPCR data represent five biological replicates of *V5::fbf-2*, four biological replicates of *csn-2(ok1288); V5::fbf-2* and *V5::fbf-2; csn-6(ok1604)*, and three biological replicates of *V5::fbf-2; csn-5(ok1064)*. Total RNA was extracted using either Monarch Total RNA miniprep kit (New England Biolabs, Cat. No. T2010S) or Direct-zol™ RNA MiniPrep kit (Zymo Research, Cat. No. R2050) as per manufacturers' protocols. RNA concentration was measured using Qubit (Thermo Fisher). cDNA was synthesized using the SuperScript IV reverse transcriptase (Invitrogen, Cat. No. 18090050) using 300 ng RNA template per each 20 µL cDNA synthesis reaction. Quantitative PCR reactions were performed in technical triplicates per each input cDNA using iQ SYBR Green Supermix (Bio-Rad, Hercules, CA, Cat. No. 1708882). Primers for *act-1* and *fbf-2* were as described (Chauve et al., 2020). Primers for *unc-54* and *fbf-1* have been previously described (Wang et al., 2020; Voronina and Seydoux, 2010). Abundance of each mRNA

in *csn* mutants [*csn-2(ok1288); V5::fbf-2, V5::fbf-2; csn-6(ok1604)*, and *V5::fbf-2; csn-5(ok1064)*] relative to wild type (*V5::fbf-2*) was calculated using comparative $\Delta\Delta\text{Ct}$ method (Plaffl, 2001) with actin *act-1* as a reference gene. After mRNA abundance of each tested gene was normalized to *act-1*, the fold change values from replicates were averaged.

Table 1

Nematode strains used in this study

Genotype	Strain Number	Reference
<i>fbf-2(q932)</i>	JK5842	Shin et al., 2017
<i>csn-2(ok1288)/hT2; fbf-2(q932)</i>	UMT 438	this study
<i>fbf-2(q932); csn-6(ok1604)/nT1</i>	UMT 439	this study
<i>fbf-2(q932); csn-5(ok1064)/nT1</i>	UMT 452	this study

Chapter Three – Results

CSN-5 interacts with FBFs

To identify proteins that might function with FBF-2, we performed a yeast two-hybrid screen with FBF-2 as bait. The screen of estimated 2×10^8 yeast diploids identified several potential FBF-2 interactors, with one of the most abundant partners being a fragment of COP9 signalosome subunit CSN-5. To validate this potential interaction and to test whether CSN-5 might interact with FBF-1 as well as with FBF-2, a targeted yeast two hybrid assay was performed by cotransforming the full-length *fbf* baits and *csn-5* prey plasmids into yeast. We observed yeast growth on the selective media, indicating binding between FBFs and CSN-5 (Figure 3.1A). Expression of c-myc tagged FBFs and HA tagged CSN-5 in yeast colonies was confirmed by western blot using anti-myc and anti-HA, respectively (Figure 3.1B). To determine if this was a direct interaction, we performed a GST pulldown assay with bacterially-expressed GST-tagged CSN-5 and His₆-tagged FBFs and detected the FBF proteins by western blot analysis with anti-His (Figure 3.1C).

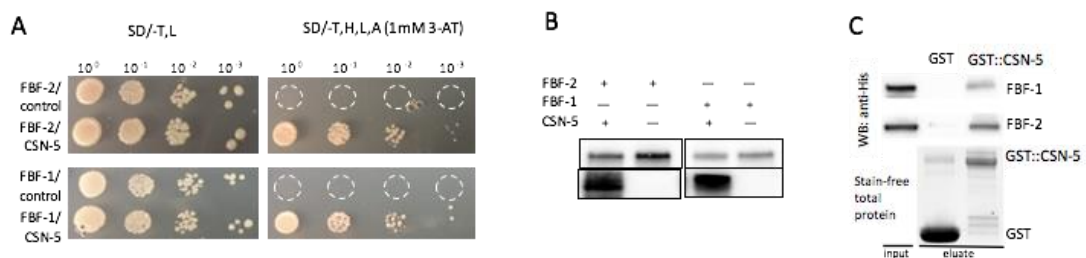


Figure 3.1. CSN-5 interacts with FBFs as discovered in yeast two hybrid assay and confirmed in GST pulldown. (A) Interaction between CSN-5 and FBF-1/-2 is detected in a yeast two-hybrid assay with FBFs as baits and CSN-5 as prey. **(B)** Western blot confirming expression of Y2H constructs. **(C)** GST pulldown assay detects a direct interaction between GST::CSN-5 and both FBF-1 and FBF-2. FBFs are detected by Western blot analysis with anti-His.

The conserved RNA-binding domain of FBFs and MPN domain of CSN-5 mediate their interaction

To elucidate the location of the interacting domains on FBFs and CSN-5, we generated several truncation constructs of FBF-1, FBF-2, and CSN-5 (Figure 3.2B,D,G), and assessed whether they interacted via GST pulldown assay detecting the proteins by western blot with anti-His and anti-GST. Interestingly, we observed that the conserved RNA-binding domain of FBFs and MPN domain of CSN-5 mediated the interaction (Figure 3.2A,C,F). Furthermore, we were able to test binding affinity of full-length CSN-5 with the FBF-2^{RBD} construct using a SPR (Biacore) assay and preliminary results indicate they bind at micromolar affinity, similar to the previously reported binding affinity of CSN5^{AC} and CSN6^{AC} constructs (Birol et al., 2014; Figure 3.2E). Since CSN-6 is the endogenous binding partner of CSN-5, the similar binding affinity suggests the interaction between FBF-2 and CSN-5 is strong enough to be physiologically relevant.

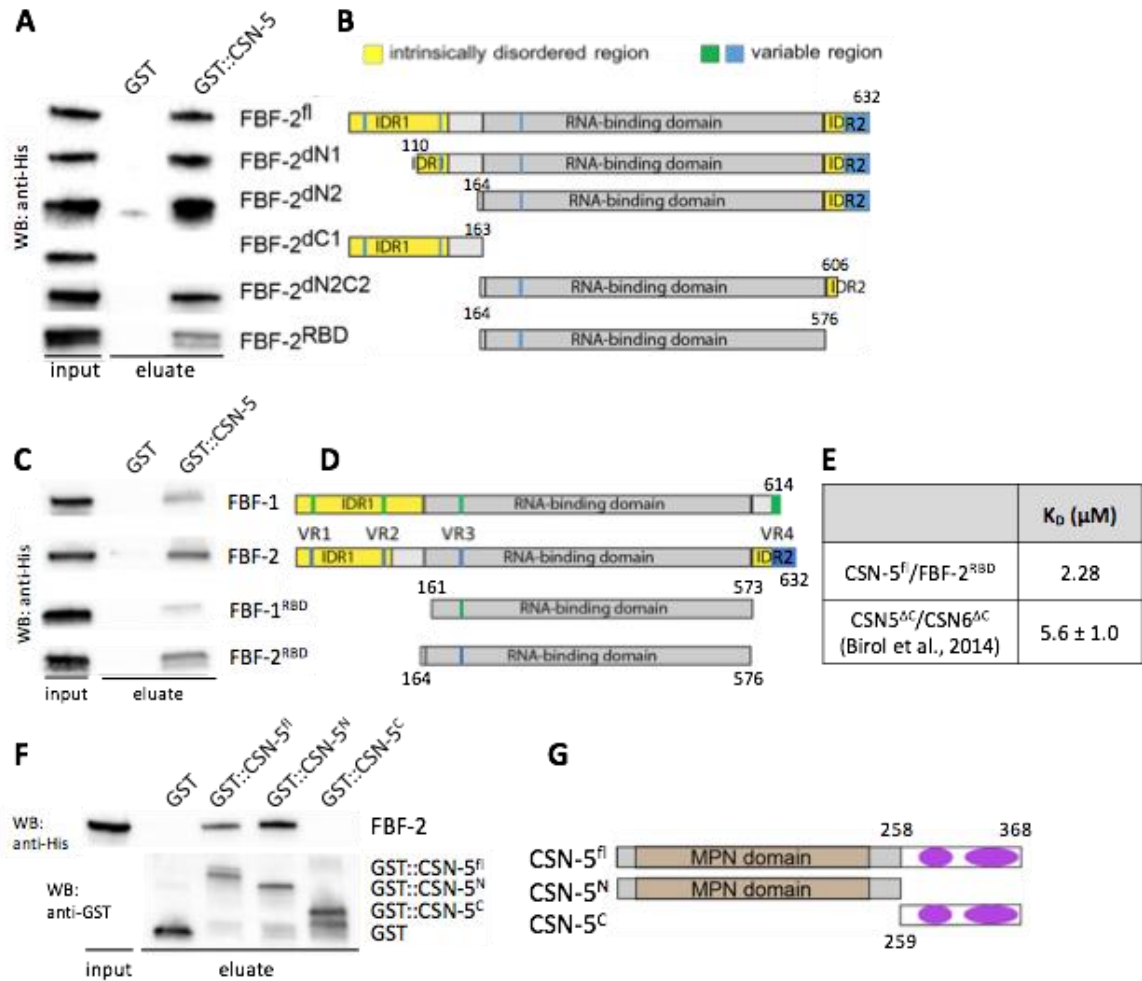


Figure 3.2. The RNA binding domain of FBFs and MPN domain of CSN-5 are sufficient for their interaction. (A) GST pull-down of GST::CSN-5 with His₆::FBF-2 constructs (B) as detected by western blot analysis with anti-His. (C) GST pull-down of GST::CSN-5 with His₆::FBF-1/2 full-length and RBD constructs (D) as detected by western blot analysis with anti-His. (E) Binding affinity of CSN-5 and FBF-2^{RBD} determined using a SPR (Biacore) assay compared to previously reported binding affinity of CSN5^{ΔC} to its endogenous binding partner CSN6^{ΔC} (Birol et al., 2014). (F) GST pull-down of GST::CSN-5 constructs (G) with His₆::FBF-2 as detected by western blot analysis with anti-His and anti-GST. Amino acid positions of protein truncations are indicated near construct schematics.

Conserved FBF-2-binding motif, KxxL, doesn't mediate binding between FBF-2 and CSN-5

Although we determined the domains on FBFs and CSN-5 which mediate this interaction, it remains unclear where the specific interacting sites are. Recently, Qiu et al.

reported a consensus binding motif KxxL found in several binding partners of FBF-2 (Qiu et al., 2019). Disruption of this sequence impairs the ability of partner proteins to bind FBF-2. Interestingly, CSN-5 contains three KxxL motifs and one is located just outside the MPN domain, spanning amino acids 231-234 (Figure 3.3B). To determine if the 231KxxL234 motif mediated binding to FBF-2, we generated three CSN-5 mutants at this position aiming to disrupt binding due to changes in amino acid size or charge. However, when we assessed binding ability via GST pulldown assay, we observed that CSN-5 231KxxL234 mutants could all still bind FBF-2 (Figure 3.3A). To verify that the two KxxL motifs in the C-terminus weren't contributing to CSN-5's binding ability, we also generated 231KxxL234 mutants for the truncated CSN-5^N construct which only had the one KxxL binding motif (Figure 3.3D). Similarly, the truncated CSN-5^N 231KxxL234 mutants were still capable of binding FBF-2 (Figure 3.3C). Therefore, although this motif may mediate binding of other partners to FBF-2 (Qiu et al., 2019), it isn't responsible for CSN-5's ability to bind FBF-2.

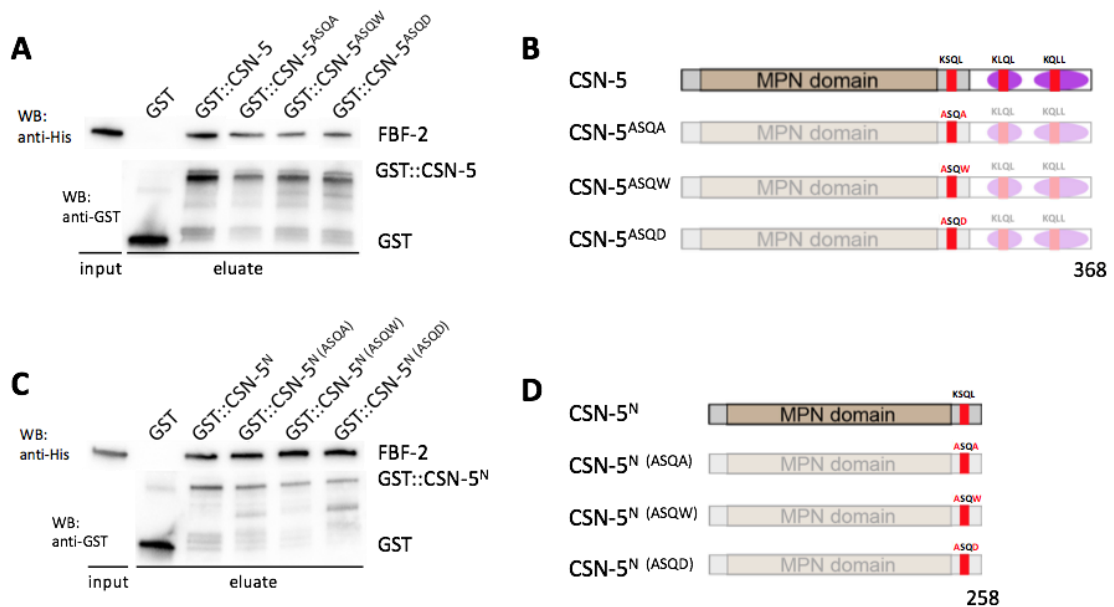


Figure 3.3. Mutating FBF-2 binding motif 231KxxL234 in CSN-5^{fl} and CSN-5^N

constructs doesn't disrupt binding. (A) GST pulldown of His₆::FBF-2 with GST::CSN-5^{fl} mutants (B) as detected by western blot analysis with anti-His and anti-GST, respectively. (C) GST pulldown of His₆::FBF-2 with GST::CSN-5^N mutants (D) as detected by western blot analysis with anti-His and anti-GST, respectively. KxxL motifs indicated by red rectangle and specific mutations indicated in red. Amino acid lengths are indicated below construct schematics.

CSN-6's MPN domain can interact with FBF-2, albeit weaker than CSN-5

Since we established the interaction between FBFs and CSN-5 was not mediated by a short linear peptide KxxL motif, we wondered if the interaction was mediated by structural recognition. Notably, another COP9 subunit, CSN-6, contains an MPN domain related to CSN-5, and since FBFs bind CSN-5's MPN domain, we wondered if FBFs could interact with CSN-6's MPN domain as well. After generating the GST::CSN-6^N construct containing its MPN domain, we performed a GST pulldown assay with His₆::FBF-2 and saw that CSN-6^N could still bind FBF-2 (Figure 3.4), although much weaker than CSN-5^N. Once the CSN-6^N protein levels were comparable to CSN-5^N levels, the interaction with FBF-2 was barely detectable, indicating that CSN-6^N can bind FBF-2 but the interaction is much weaker than what we see with CSN-5^N.

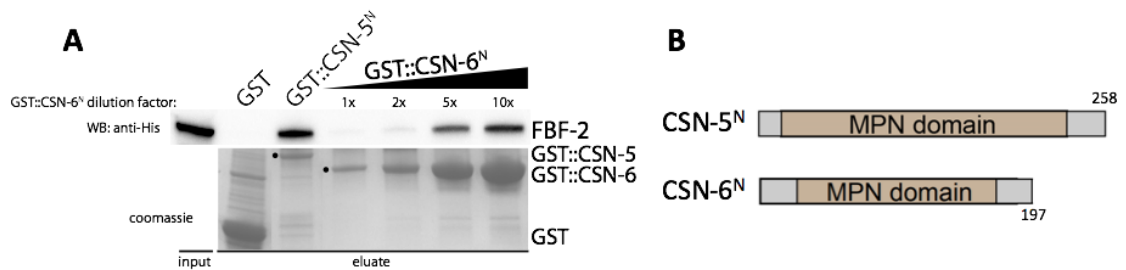


Figure 3.4. CSN-6 weakly associates with FBF-2. (A) GST pulldown assay of His₆::FBF-2 with GST::CSN-5^N or GST::CSN-6^N constructs (B) at increasing protein concentrations as detected by western blot analysis with anti-His. Total protein is seen by coomassie. Amino acid lengths are indicated by construct schematics.

CSN-5 does not help CSN-6 bind FBF-2

Next, we wondered if a complex of CSN-5 and CSN-6 would be able to bind to FBF-2. Since CSN-5 must dimerize with CSN-6 to be incorporated into the COP9 signalosome complex (Birol et al., 2014), the ability of CSN-5 to interact with FBF-2 while bound to CSN-6 would suggest that FBF-2 might form a complex with the whole COP9 signalosome. To answer this question, we performed GST pulldown assays of His₆::FBF-2 with GST::CSN-6^N dilutions, with or without the addition of FLAG₃::CSN-5^N. We saw no difference in the ability of CSN-6^N to bind FBF-2 with or without the addition of CSN-5^N (Figure 3.5), suggesting that the interaction between FBFs and CSN-5 may take place outside of the COP9 signalosome complex.

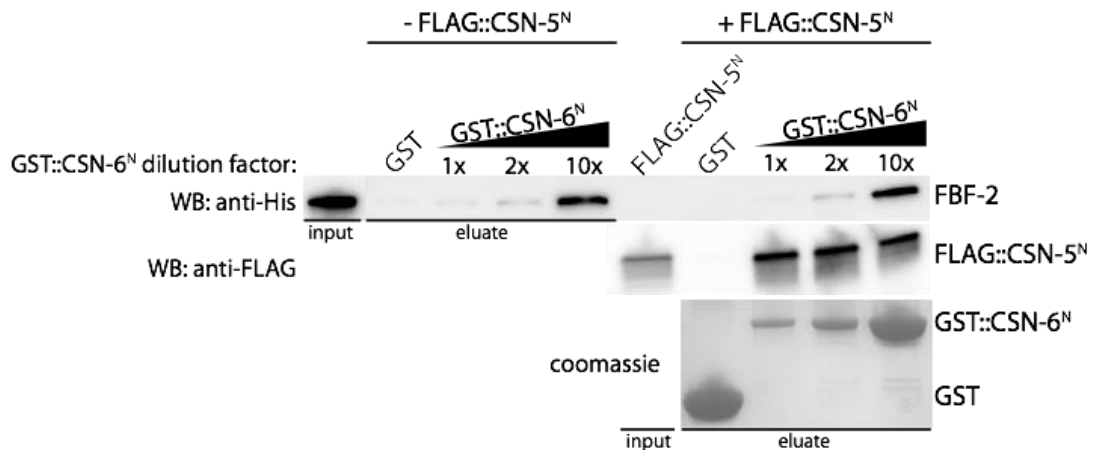


Figure 3.5. CSN-5 doesn't help CSN-6 bind FBF-2. GST pulldown assay of His₆::FBF-2 with GST::CSN-6^N dilutions, with or without the addition of FLAG₃::CSN-5^N as detected by western blot analysis with anti-His or anti-FLAG and coomassie to visualize GST alone and GST::CSN-6^N.

FBF-2 binding with CSN-5/-6 is unaffected by RNase treatment

Conformations of RNA-binding proteins such as FBFs might change upon binding to their target mRNAs and these conformational differences might affect FBFs' ability to

interact with their protein partners. Alternatively, MPN domain of CSN-5 and CSN-6 might have unappreciated RNA-binding activity and form a complex with an FBF target mRNA rather than with FBF proteins directly. Therefore, we were curious if FBFs' interaction with CSN-5 and CSN-6 were RNA-dependent. To address this question, we conducted GST pulldown assays of FBF-2 and CSN-5/-6 with or without depleting RNAs in the lysates by the addition of RNase. We found that the FBF-2 binding to CSN-5/-6 was not affected by RNase treatment (Figure 3.6), indicating that this interaction is likely not RNA-dependent.

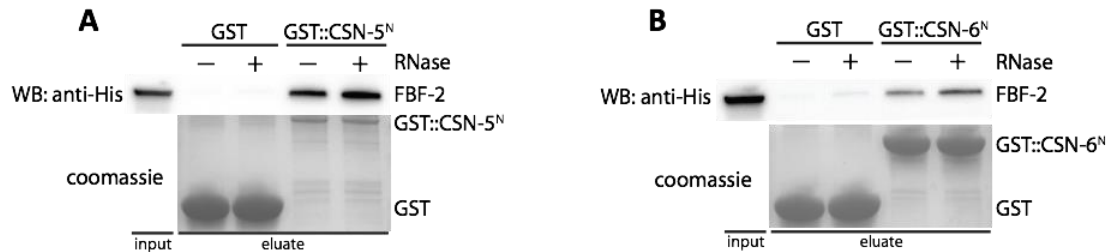


Figure 3.6. RNase treatment does not affect FBF-2 binding with CSN-5 or CSN-6. GST pulldown assay of His₆::FBF-2 with (A) GST::CSN-5^N or (B) GST::CSN-6^N with or without RNase treatment. FBF-2 protein is detected by western blot analysis with anti-His. GST alone or GST tagged constructs detected by coomassie.

Conserved domains of human homologs PUM1 and CSN5 also interact

Notably, both FBFs and CSN-5 have homologous human proteins, PUM1/PUM2 and CSN5, respectively. Since we determined that region of interaction was within evolutionarily conserved structured domains, the RNA-binding domain of FBFs and MPN domain of CSN-5, we wanted to further investigate if this interaction was conserved in the respective human homologs. We generated His₆::PUM1^{HD} and GST::CSN5^N constructs which contained the regions homologous to FBFs' RNA-binding domain and CSN-5's MPN domain, respectively. A GST pulldown assay with the

GST::CSN5^N His₆::PUM1^{HD} revealed that the interaction we observed for the nematode proteins is conserved for homologous human proteins, indicating an evolutionarily conserved interaction (Figure 3.7).

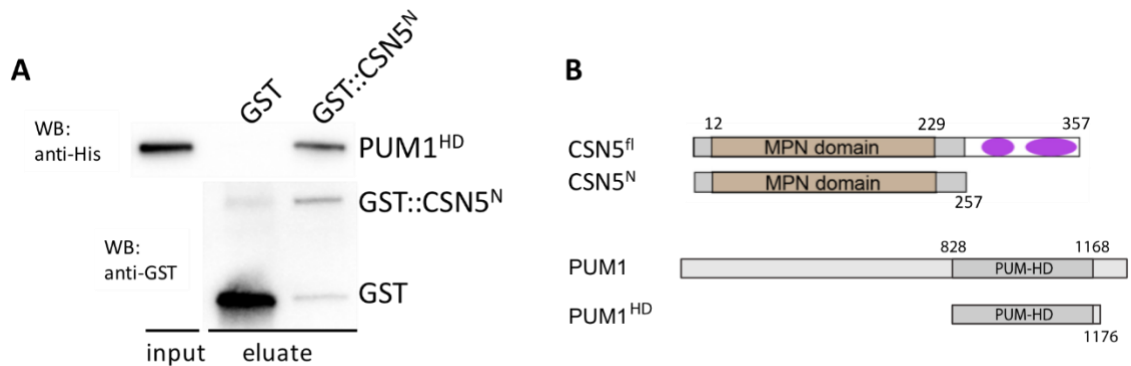


Figure 3.7. Human homologs PUM1 and CSN5 also directly interact. (A) GST pull-down of GST::CSN5^N with His₆::PUM1^{HD} as detected by western blot analysis with anti-His and anti-GST. **(B)** Schematics of full-length CSN5 and PUM1 with their respective truncation constructs. Amino acid lengths of protein constructs indicated near construct schematics.

COP9 subunit mutants have reduced number of stem cells and both mutants of *csn-5* and *csn-6* exhibit masculinization of germline phenotype

Since the COP9 signalosome (CSN) has roles in regulating protein stability and CSN-5 has been known to interact with other cellular proteins and may have interactions independent of the COP9 complex (Tomoda et al., 2005; Shackleford and Claret, 2010; Yoshida et al., 2013), we wondered if the signalosome or CSN-5 uniquely were facilitating FBF function in the germline. Because FBF-1/2 regulate the switch from mitosis to meiosis in the *C. elegans* germline (Zhang et al., 1997; Crittenden et al., 2002; Wickens et al., 2002; Wang and Voronina, 2020) and therefore affect the size of its stem and progenitor cell (SPC) population, we quantified the number of stem cells in several *csn* mutant strains: *csn-2(ok1288)*, *csn-5(ok1064)*, and *csn-6(ok1604)*. We dissected and stained adult germlines with the antibodies to a stem cell marker, REC-8, to visualize the

SPC zone and DAPI to visualize DNA (Figure 3.8Bi-iv). Compared to the wild type, we observed all *csn* loss of function (*lf*) mutants had reduced numbers of stem cells (Figure 3.8A, $p < 0.0001$) which is in general agreement with previously reported work (Brockway et al., 2014). The *csn-6(ok1604)* and *csn-5(ok1064)* mutants had the most drastic reduction in SPCs, whereas the *csn-2(ok1288)* SPCs were affected comparatively weakly (Figure 3.8A, $p < 0.01$). This decrease in SPCs we observed may be consistent with a decrease in FBF function. Furthermore, FBFs play a role in sex determination by regulating the spermatogenesis to oogenesis switch (Crittenden et al., 2002), so next we assessed if sex determination was affected in the *csn* subunit mutants. Interestingly, the majority of *csn-6(ok1604)* and *csn-5(ok1064)* mutants exhibited a masculinization of germline (Mog) phenotype where only sperm is produced and no oocytes (Table 2, Figure 3.8Ciii-iv). This Mog phenotype is also seen in *fbf-1/-2(lf)* strains (Crittenden et al., 2002), supporting the hypothesis that *csn* is contributing to FBF function. Curiously, the *csn-2(ok1288)* mutant had clearly distinct phenotypes where most germlines could still form oocytes (Table 2, Figure 3.8Cii). We conclude that CSN-5 can facilitate FBFs' functions in stem cell maintenance and sex determination since *csn-5(lf)* results in reduced stem cell numbers and mostly Mog phenotype. This new role for CSN-5 also appears to be mediated by CSN-5 alone, rather than the complete COP9 signalosome complex. If the whole complex were required to facilitate FBFs' functions, we would expect to see the same, or very similar, phenotypes among all *csn(lf)* mutants. Taken together with SPC quantification, the distinct phenotypes we see in the *csn-2(ok1288)* mutant indicate that *csn-5(ok1064)* is affecting *fbf* function independently of the signalosome.

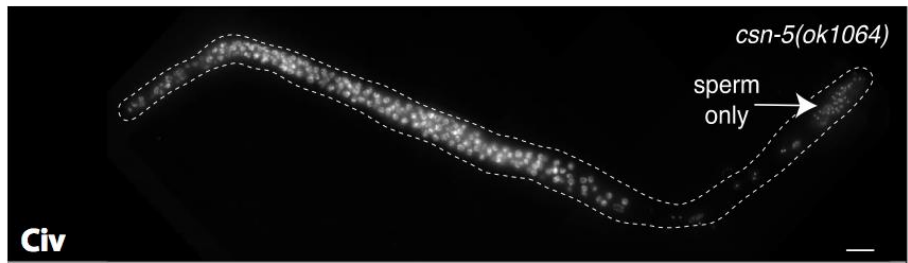
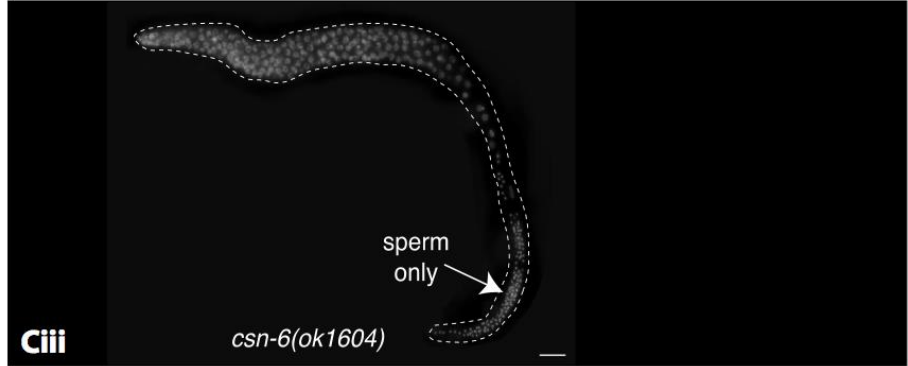
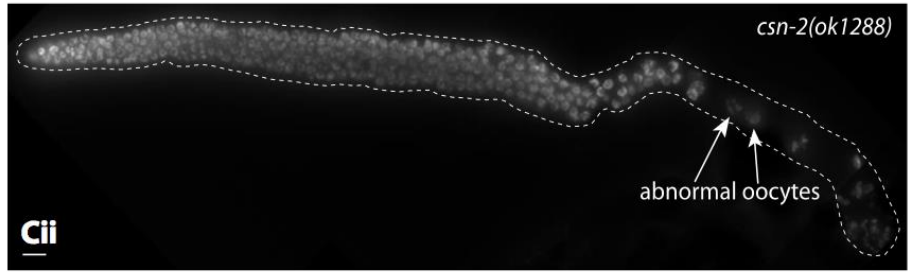
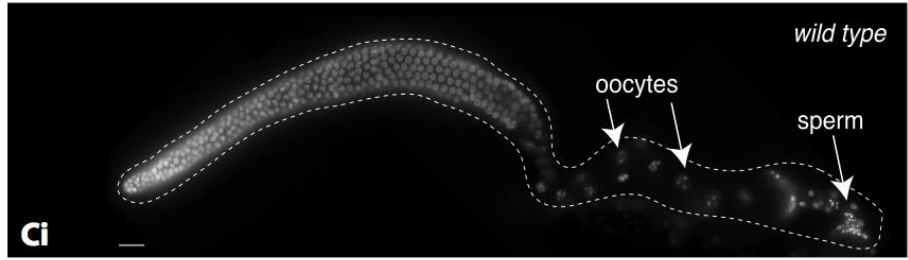
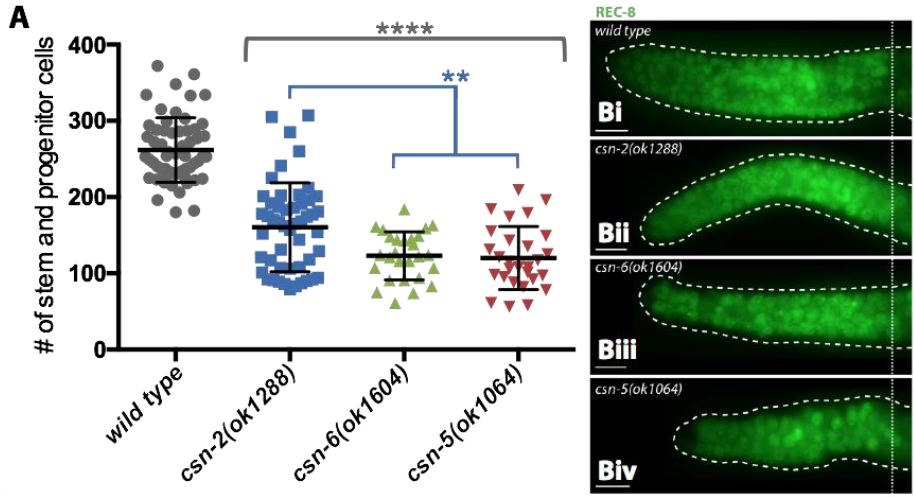


Figure 3.8. Phenotypic analysis of *csn* mutants reveals reduced number of stem cells and mutants of *csn-5* and *csn-6* exhibit *fbf-1/2(lf)* phenotype. (A) Quantification of stem and progenitor cell (SPC) number in wild type and *csn* mutant worms listed. Differences in number of SPCs was evaluated by one-way ANOVA with Tukey's post-test. All mutants exhibited a reduction in stem cell numbers compared to wild type (****, $p < 0.0001$). *csn-5* and *csn-6* mutants have the most drastic reduction in stem cells, which may be consistent with decrease in FBF function, whereas *csn-2* mutants were not as affected as *csn-5* or *csn-6* (**, $p < 0.01$). (Bi-iv) Distal germlines dissected from adult wild type and respective *csn* mutants were stained with anti-REC-8 (green) to visualize SPC zone. Gonads of adult wild type and respective *csn* mutants are dissected and stained for DNA with DAPI (Ci-iv). Mutants of *csn-6* (Ciii) and *csn-5* (Civ) exhibit a masculinization of germline (Mog) phenotype in which only sperm is produced similar to that seen in *fbf-1/2(lf)*, whereas the *csn-2* mutant displays a distinctly different phenotype where oocytes can still form. Arrows indicate gametes. Scale bars: 10 μ m.

Genotype	% abnormal oocytes	% Mog	% no gametes	<i>n</i>
wild type	0	0	0	127
<i>csn-2(ok1288)</i>	75	3.9	9.2	76
<i>csn-6(ok1604)</i>	25.8	70.8	1.7	120
<i>csn-5(ok1064)</i>	7.9	82.5	9.5	63

n indicates number of germlines scored. Mog is masculinization of germline phenotype characterized by sperm only (no oocytes). Mog is a *fbf-1/2* double mutant phenotype.

***csn(lf)* causes a decrease of FBF-1/2 protein levels**

In *C. elegans*, CSN-5 was previously identified as an interacting partner of germline proteins, GLH-1 and GLH-3 (Smith et al., 2002), and found to promote accumulation of GLH-1 (Orsborn et al., 2007). Therefore, we hypothesized that CSN-5 by itself or with other COP9 subunits facilitates FBF function by promoting FBF accumulation. We tested this hypothesis by quantifying FBF protein levels in the *csn* mutant worm lysates using anti-tubulin, anti-FBF-1, and anti-V5 to detect tubulin as a loading control, FBF-1, and V5-tagged FBF-2. We found a reduction in total FBF-1 protein level in *csn* mutants compared to wild type, and this reduction was only statistically significant in the *csn-5(lf)* mutant ($p < 0.01$; Figure 3.9A). We confirmed this reduction in FBF-1 by immunostaining the *csn* mutants and visualizing the loss in the distal stem cells (Figure 3.9B), where

FBFs are normally expressed. The stronger FBF-1 protein reduction in *csn-5(lf)* implies that CSN-5 might be promoting the accumulation of FBF-1 independently of the complex, since the relative amounts of FBF-1 would be similar if CSN-5's effects were dependent upon its incorporation into the COP9 complex. Furthermore, we observed a significant reduction of V5::FBF-2 in *csn-6(lf)* and *csn-2(lf)* mutants by western blot ($p < 0.005$ and $p < 0.01$, respectively; Figure 3.9C) and confirmed this observation by immunostaining the mutants (Figure 3.9D).

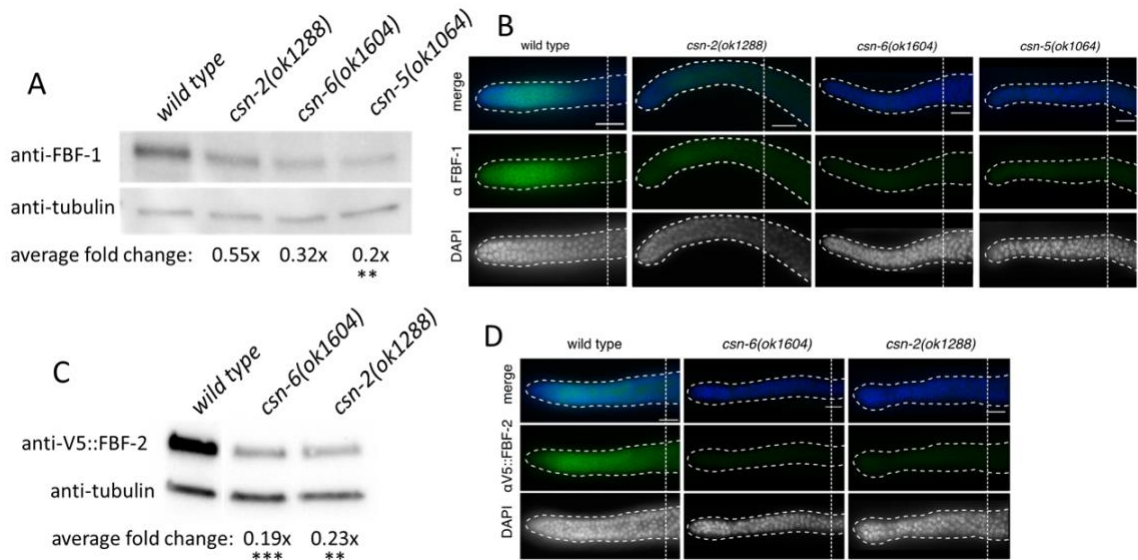


Figure 3.9. FBF-1/2 protein levels are reduced in *csn(lf)* mutants. Western blot analysis of *csn(lf)* mutant worm lysate reveals reduced levels of (A) FBF-1, and (C) V5::FBF-2. Tubulin is used as a loading control, detected by anti-tubulin. FBF-1 and FBF-2 are detected by anti-FBF-1 and anti-V5, respectively. Gonads of *csn(lf)* mutants are dissected and stained with (B) anti-FBF-1 or (D) anti-V5 with DAPI to visualize protein levels of FBF-1/2. Differences in total FBF protein level between *csn(lf)* mutants and wild type was evaluated by one-way ANOVA with Dunnett's post-test (**, $p < 0.01$; ***, $p < 0.005$). Scale bar: 10 μ m.

Cannot exclude *csn(lf)* effects on *fbf* transcript levels

Since *csn(lf)* reduced FBF-1/2 protein levels, we next tested if *csn(lf)* might affect *fbf-1/-2* mRNA as well. To determine if *csn* mutants were affecting *fbf* mRNA levels, we

evaluated relative *fbf* mRNA abundance in *csn(lf)* mutant strains using quantitative PCR. Using *unc-54* (myosin heavy chain) as a control and normalizing mRNA abundance to a reference gene, *act-1* (actin), we observed a reduction in *fbf-1* mRNA abundance in each of the mutants but there was too much variability in our technical and biological replicates to find a significant difference. However, we observed a statistically significant reduction of *fbf-2* relative mRNA abundance in the *csn-2(ok1288)*, *csn-6(ok1604)*, and *csn-5(ok1064)* loss of function mutants compared to wild type (Figure 3.10, $p < 0.0001$) and therefore we cannot exclude the possibility that the decrease in FBF-1/2 protein levels in *csn(lf)* mutants results from a decrease in their transcript levels.

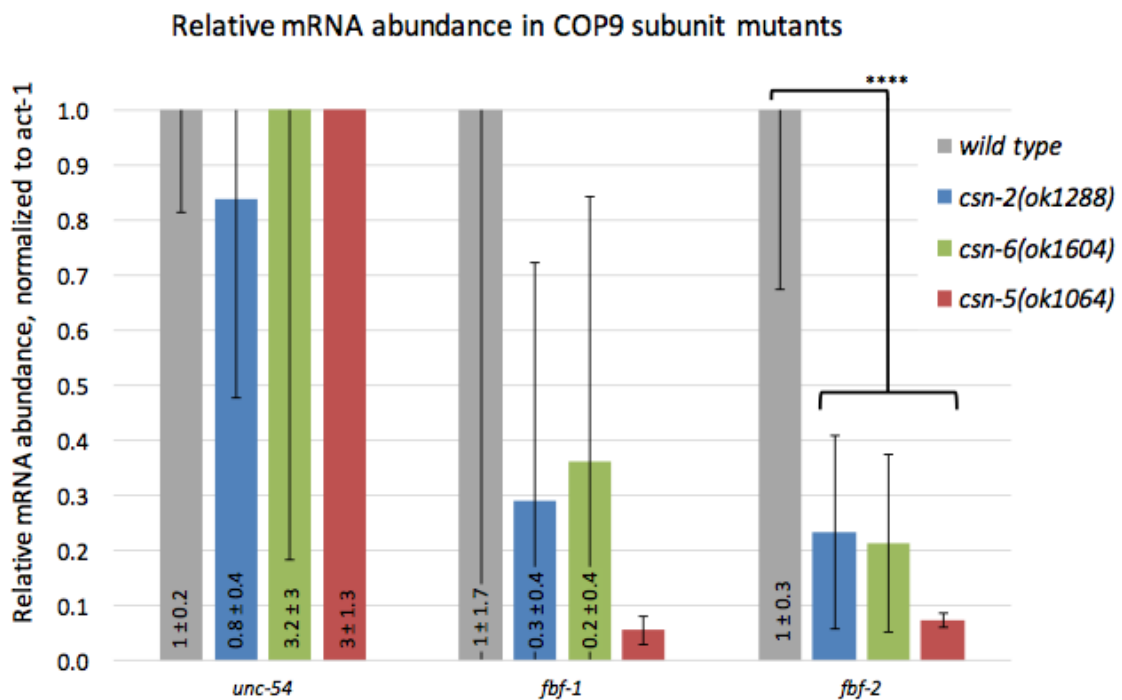


Figure 3.10. Relative mRNA abundance of *fbf-2* is reduced in *csn-2(ok1288)*, *csn-6(ok1604)*, and *csn-5(ok1064)* loss of function mutant worms (RT-qPCR). mRNA abundance is normalized to reference gene *act-1*, and *unc-54* were used as a loading control. Differences in relative mRNA abundance of *fbf-2* was evaluated by one-way ANOVA with Tukey's post-test. All mutants exhibited a reduction of *fbf-2* mRNA compared to wild type (****, $p < 0.0001$).

Chapter Four – Discussion and Future Prospects

CSN-5's novel interaction with FBF-1 and FBF-2

In this study, we have identified a new interacting partner of PUF-family RNA-binding proteins, the COP9 signalosome component CSN-5. We found that this direct interaction is mediated by conserved structured domains, FBFs' RNA-binding domain and CSN-5's MPN domain (Figure 3.2C,F). Additionally, we've shown that this interaction is evolutionarily conserved, as this novel interaction is also seen in corresponding human homologs PUM1 and CSN5 (Figure 3.7). Furthermore, our preliminary binding affinity data suggests this interaction may be biologically relevant, since full-length CSN-5 binds FBF-2^{RBD} at micromolar affinity (Figure 3.2E) similar to the previously described binding affinity of CSN-5^{ΔC} with its binding partner CSN-6^{ΔC} (Birol et al., 2014).

We were also curious to see how this interaction was mediated, since some FBF-2-interacting proteins utilize short linear peptide motifs to associate with FBF-2's RNA-binding domain (Qiu et al., 2019). Although mutating a reported FBF-2 KxxL binding sequence (Qiu et al., 2019) also found in CSN-5 didn't seem to disrupt binding (Figure 3.3), we were able to gain some insight when exploring the structural recognition route. CSN-6 also contains an MPN domain similar to CSN-5 (Birol et al., 2014; Lingaraju et al., 2014), making CSN-6 an excellent candidate to test the hypothesis that the interaction may be mediated by structural recognition. We observed that CSN-6's MPN domain could bind FBF-2's RNA-binding domain, but only at much higher concentrations than CSN-5 (Figure 3.4). This could indicate that although these conserved domains appear to mediate the interaction, specific amino acids within these domains determine the strength of the interaction.

CSN-5 promotes FBFs function and accumulation independent of the COP9 signalosome

The COP9 signalosome's most studied function is as a regulator of protein degradation (Wei et al., 1994; Chamovitz et al., 1996; Claret et al., 1996; Chamovitz, 2009); however, its component CSN5 has been shown to interact with and promote the accumulation of other cellular proteins independently of the COP9 complex (Smith et al., 2002; Tomoda et al., 2005; Orsborn et al., 2007; Shackleford and Claret, 2010; Yoshida et al., 2013). Here, we have shown FBFs protein levels are reduced in *csn-5(lf)* mutant compared to wild type (Figure 3.9), suggesting that CSN-5 can promote the accumulation of FBFs thereby allowing for proper FBF function. We have also shown that *csn-5(lf)* mutants result in decreased numbers of stem cells and a failure to properly switch from spermatogenesis to oogenesis during differentiation (Figure 3.8), consistent with loss in FBFs function. Furthermore, we hypothesize that CSN-5's effects on FBFs are independent of the COP9 complex and are the workings of CSN-5 alone. This conclusion is supported by three lines of evidence. First, we see that stem cell numbers and sex determination phenotypes are distinct between *csn-2(lf)* and *csn-5(lf)* mutants (Figure 3.8). Second, we observed differences in total FBF-1 protein level in the *csn-2(lf)* mutant compared to *csn-5(lf)* (Figure 3.9), indicating CSN-5's effects on FBF are independent of the complex, otherwise, our observations should be similar among all *csn(lf)* mutants. Third, since CSN-5 must dimerize with CSN-6 to be incorporated into the COP9 complex (Birol et al., 2014), we tested if the complex of CSN-5 with CSN-6 would bind FBF-2. Interestingly, we saw that the CSN-5/-6 complex did not improve CSN-6's binding to FBF-2 as there was no difference seen with or without the addition of CSN-5 (Figure

3.5), which further indicates CSN-5 may be functioning independently outside of the COP9 complex.

We propose that CSN-5 promotes the accumulation of FBFs, which in turn allows for their proper function in stem cell maintenance and regulating the spermatogenesis-to-oogenesis switch, either directly or indirectly. Because we observed a statistically significant reduction of *fbf-2* relative mRNA abundance in the *csn(lf)* mutants compared to the wild type (Figure 3.10, $p < 0.0001$), we cannot exclude the possibility that the decrease in FBF-1/2 protein levels in *csn(lf)* mutants results from indirect effects such as from a decrease in their transcript levels.

Implications for human cancers

Since CSN5 is known to be overexpressed in several human cancers (Figure 1.2; Lee et al., 2011), we are curious if the overexpression of CSN-5 would promote tumor formation in the worm germline. This would provide more insight on the role of CSN5 in human cancer pathophysiology. Additionally, the COP9 signalosome's most studied mechanism of regulating protein degradation is by deneddylation (Cope et al., 2002; Lingaraju et al., 2014) and the process of neddylation has been shown to modulate tumorigenesis (Zhou et al., 2019). Notably, a novel NEDD8-activating enzyme inhibitor, pevonedistat, was clinically efficacious in phase 2 trials (Sekeres et al., 2021) and is currently in phase 3 clinical trials for patients with myelodysplastic syndrome and acute myeloid leukemia. The utilization of this NEDD8-activating enzyme inhibitor as a chemotherapeutic further validates the role of the neddylation signaling pathway in cancer pathophysiology. Furthermore, it is possible that deneddylation may be a mechanism by which CSN-5 promotes the accumulation and function of FBFs as

Brockway et al. showed that *ned-8(RNAi)* partially suppressed defects seen in *csn* mutants (Brockway et al., 2014). Aside from the roles of CSN5 in cancer physiology, precise control of FBFs/PUMs are also necessary for stem cell maintenance and prevention of tumorigenesis (Kedde et al., 2010; Kalchhauser et al., 2011; Miles et al., 2012; Guan et al., 2018; Wang et al., 2020; Gor et al., 2021; Shi et al., 2021; Smialek et al., 2021) which makes this investigation of CSN-5 and FBFs especially interesting for better understanding of cancer physiology. Excitingly, Schlierf et al. has generated a CSN5 inhibitor which has been shown to inhibit tumor growth (Figure 1.3; Schlierf et al., 2016) and since we established here that human homologs CSN5 and PUM1 interact *in vitro* (Figure 3.7), we are curious if PUM levels are affected in CSN5 inhibitor-treated mammalian cells. Investigating the relationship between CSN-5/CSN5 and FBFs/PUMs is an exciting new avenue for better understanding their roles in tumorigenesis and the applications toward human cancers.

Future Directions

Here, we have identified a novel interaction between stem cell regulators, FBF-1 and FBF-2, and cancer-associated protein CSN-5. We plan to continue investigating various aspects of this novel interaction with specific questions in mind. First, which specific residues mediate the interaction between FBFs/PUM1's RNA-binding domain and CSN-5/CSN5's MPN domain? These might be identified by comparing common amino acid sequences within the homology domain/RNA-binding domain between PUM1, FBF-1, and FBF-2 that are not shared with PUM2 since we have preliminary data showing that PUM2 does not bind CSN5 *in vitro*. We can also compare common sequences within the

MPN domain between human CSN5, worm CSN-5, and human EIF3F, another protein whose MPN domain interacts with PUM1 as indicated by some of our preliminary results. We can then map the conserved amino acid sequences onto the 3D structures of the respective homology/RNA-binding domains or MPN domains to identify exposed sequences that would be more accessible to facilitate protein-protein interactions. Second, is this interaction observed *in vivo*? We are currently addressing this question by utilizing a proximity ligation assay (PLA). Our preliminary results indicate that CSN-5 and FBFs are within close proximity (<40 nm) of each other in the worm germline which may indicate they can interact *in vivo*. Third, is this interaction truly RNA-independent? We have concluded that this interaction does not depend on RNA by GST pulldown with or without addition of RNase to deplete RNAs in the lysates (Figure 3.6). However, there exists the possibility that RNA binding proteins, such as FBFs, can protect the RNA such that RNases are unable to access and cleave it. To determine if this interaction is truly RNA-independent, one option could be to mutate specific residues within FBFs' RNA-binding domain that are essential for RNA-binding (Bernstein et al., 2005), and see if CSN-5/-6 binding remains unaffected. Fourth, does CSN-6 compete with FBF-2 for binding with CSN-5? Or conversely, does FBF compete with CSN-6 for binding with CSN-5? Since we demonstrated here that CSN-6 binds FBF-2 much more weakly than CSN-5 (Figure 3.4), and our preliminary binding affinity data suggests that CSN-5 binds FBF-2 with a similar affinity to that of CSN-5 binding to its partner CSN-6 (Figure 3.2E), we wonder if there may be a molecular "tug-of-war" going on between CSN-5, CSN-6, and FBFs. To better understand the relationship between CSN-5, CSN-6, and FBFs, we

could conduct a binding assay with constant versus titrated amounts of purified proteins similar to that which has been previously described (Menichelli et al., 2013).

We are also excited to explore different avenues regarding the biological relevance of this interaction with specific questions in mind. First, what do the FBF-2 protein levels look like in the *csn-5(lf)* mutant? We are currently conducting experiments to answer this question, and preliminary results reveal that FBF-2 protein levels are depleted in the *csn-5(lf)* mutant, but total protein levels may not be much different than *csn-6(lf)* and *csn-2(lf)* mutants. We then ask, why might all mutants have similar levels of FBF protein reduction, but exhibit distinctly different phenotypes? One possibility might be that there are post-translational modifications occurring which may impact protein functionality. Second, is the reduction in FBFs protein levels indirect and due to reduction in their respective transcripts? Interestingly, we have shown that *fbf-2* transcript is significantly reduced in the *csn(lf)* mutants (Figure 3.10). To differentiate between protein degradation versus lack of new transcription, we could treat the *csn(lf)* mutants with a proteasome inhibitor or NEDD8-activating enzyme inhibitor to block protein degradation, and then assess FBF protein levels in the *csn(lf)* mutants. If we don't observe a difference in total protein levels after treatment, it may indicate that the COP9 signalosome affects FBF protein levels through mRNA transcription. Another option could be to conduct a pulse-chase experiment to measure protein degradation in real time. Third, what might be the mechanism by which CSN-5 promotes FBFs' accumulation and function? Deneddylation is the COP9 complex's most studied mechanism by which it regulates protein degradation (Cope et al., 2002; Lingaraju et al., 2014) and *ned-8(RNAi)* has been shown

to partially suppress defects seen in *csn(lf)* mutants (Brockway et al., 2014). Therefore, we speculate that deneddylation might also be how CSN-5 promotes the accumulation and function of FBFs. We can perform *ned-8(RNAi)* experiments on the *csn(lf)* mutants to determine if number of SPCs and oogenesis is restored. We might also harvest these RNAi-treated worms for western blot to see if FBFs levels are different than what we have reported here (Figure 3.9). Another approach could be to treat the *csn(lf)* mutants with a NEDD8-activating enzyme inhibitor and similarly see if number of SPCs and oogenesis is restored. Alternatively, we could also mutate the catalytic isopeptidase residues within CSN-5's MPN domain to ablate its deneddylating activity, then incorporate this mutation in the worm to see if we observe phenotypes which mimic what we report here (Figures 3.8, 3.9). Any of these options might provide insight on if deneddylation is a mechanism by which CSN-5 promotes FBFs accumulation and function. Fourth, is CSN-5's role in FBFs' function truly independent of the COP9 complex? Here, we have demonstrated that CSN-5 is likely functioning independently (Figures 3.5, 3.8, 3.9). To further test our hypothesis that CSN-5 is functioning independently of the COP9 complex, we will be incorporating a CSN-5^N transgene into a *csn-5(lf)* mutant background to determine if oogenesis and/or stem cell numbers can be rescued. Since this transgenic construct doesn't contain the C-terminal domain that integrates into the COP9 complex (Birol et al., 2014; Lingaraju et al., 2014), we would be able to see the effects of CSN-5 alone without rescuing full COP9 function. If *csn-5* functions independently of COP9 complex, why does *csn-6(lf)* mutation lead to germline phenotypes similar to those caused by *csn-5(lf)*? One explanation may be that CSN-5 is destabilized and is thus less abundant in the *csn-6(lf)* mutant. We have begun testing this

theory, and our preliminary results indicate that CSN-5 protein levels are indeed reduced in the *csn-6(lf)* mutant, which may account for why we observed similar findings with the *csn-6(lf)* mutant as the *csn-5(lf)* mutant. This situation can also be remedied by incorporating the CSN-5^N transgene into the *csn-6(lf)* mutant background to restore CSN-5 function while still observing the effects of the *csn-6(lf)* mutant. We would then expect to see phenotypes similar to *csn-2(lf)* mutant if the phenotypes we see in our current *csn-6(lf)* mutant are truly due its depletion of *csn-5*. Fifth, does overexpression of CSN-5 promote germline tumor formation? Since CSN5 is overexpressed in several human cancers (Figure 1.2; Lee et al., 2011), we wonder if the overexpression of CSN5 itself promotes tumor formation. We plan to overexpress CSN-5 in a worm strain predisposed to germline tumors and test if CSN-5 overexpression results in increased tumor formation. Lastly, what happens to human PUM protein levels in mammalian cells when a CSN5 inhibitor is administered? As we know that both PUMs and CSN5 play roles in human cancers, we are excited to further investigate the relationship between them and how it might influence tumorigenesis in humans. Since there is a CSN5 inhibitor available, we are curious to see if PUM levels are affected in mammalian cells when treated with the drug. Understanding the connection between CSN5 and PUMs could provide insight on the molecular mechanisms of cancer pathophysiology in humans.

References

1. Bernstein D, Hook B, Hajarnavis A, Opperman L, Wickens M. Binding specificity and mRNA targets of a *C. elegans* PUF protein, FBF-1. *RNA* 2005;11(4):447-458.
2. Birol M, Enchev RI, Padilla A, Stengel F, Aebersold R, Betzi S, Yang Y, Hoh F, Peter M, Dumas C, Echalié A. Structural and biochemical characterization of the Cop9 signalosome CSN5/CSN6 heterodimer. *PLoS One* 2014;9(8):e105688.
3. Blagosklonny MV. Target for cancer therapy: proliferating cells or stem cells. *Leukemia* 2006;20(3):385-391.
4. Brenner S. The genetics of *Caenorhabditis elegans*. *Genetics* 1974;77(1):71-94.
5. Brockway H, Balukoff N, Dean M, Alleva B, Smolikove S. The CSN/COP9 signalosome regulates synaptonemal complex assembly during meiotic prophase I of *Caenorhabditis elegans*. *PLoS Genet* 2014;10(11):e1004757.
6. Buck SH, Chiu D, Saito RM. The cyclin-dependent kinase inhibitors, cki-1 and cki-2, act in overlapping but distinct pathways to control cell-cycle quiescence during *C. elegans* development. *Cell Cycle* 2009;8(16):2613-2620.
7. Chagastelles PC, Nardi NB. Biology of stem cells: an overview. *Kidney Int Suppl* 2011;133(3):63-67.
8. Chamovitz DA, Wei N, Osterlund M, et al. The COP9 complex, a novel multisubunit nuclear regulator involved in light control of a plant developmental switch. *Cell* 1996;86(1):115-121.
9. Chamovitz DA. Revisiting the COP9 signalosome as a transcriptional regulator. *EMBO Rep* 2009;10(4):352-358.
10. Chauve L, Le Pen J, Hodge F, et al. High-throughput quantitative RT-PCR in single and bulk *C. elegans* samples using nanofluidic technology. *J Vis Exp* 2020;(159):10.3791/61132.
11. Claret FX, Hibi M, Dhut S, Toda T, Karin M. A new group of conserved coactivators that increase the specificity of AP-1 transcription factors. *Nature* 1996;383(6599):453-547.
12. Cope GA, Suh GSB, Aravind L, et al. Role of predicted metalloprotease motif of Jab1/Csn5 in cleavage of Nedd8 from Cul1. *Science* 2002;298(5593):608-611.
13. Crittenden SL, Bernstein DS, Bachorik JL, et al. A conserved RNA-binding protein controls germline stem cells in *Caenorhabditis elegans*. *Nature* 2002;417(6889):660-663.
14. Day NJ, Wang X, Voronina E. In Situ Detection of Ribonucleoprotein Complex Assembly in the *C. elegans* Germline using Proximity Ligation Assay. *J Vis Exp* 2020;(159):10.3791/60982.
15. Echalié A, Pan Y, Birol M, et al. Insights into the regulation of the human COP9 signalosome catalytic subunit, CSN5/Jab1. *Proc Natl Acad Sci USA* 2013;110(4):1273-1278.
16. Ellenbecker M, Osterli E, Wang X, et al. Dynein Light Chain DLC-1 Facilitates the Function of the Germline Cell Fate Regulator GLD-1 in *Caenorhabditis elegans*. *Genetics* 2019;211(2):665-681.

17. Enane FO, Sauntharajah Y, Korc M. Differentiation therapy and the mechanisms that terminate cancer cell proliferation without harming normal cells. *Cell Death Dis* 2018;9(9):912.
18. Goldstrohm AC, Hall TMT, McKenney KM. Post-transcriptional regulatory functions of mammalian pumilio proteins. *Trends Genet* 2018;34(12):972-990.
19. Gor R, Sampath SS, Lazer LM, Ramalingam S. RNA binding protein PUM1 promotes colon cancer cell proliferation and migration. *Int J Biol Macromol* 2021;174:549-561.
20. Guan X, Chen S, Liu Y, Wang L, Zhao Y, Zong Z. PUM1 promotes ovarian cancer proliferation, migration and invasion. *Biochem Biophys Res Commun* 2018;497(1):313-318.
21. Hansen D, Hubbard EJA, Schedl T. Multi-pathway control of the proliferation versus meiotic development decision in the *Caenorhabditis elegans* germline. *Dev Biol* 2004;268(2):342-357.
22. Hofmann K, Bucher P. The PCI domain: a common theme in three multiprotein complexes. *Trends Biochem Sci* 1998;23(6):204-205.
23. Hubbard EJA. The *C. elegans* germ line: a model for stem cell biology. *Dev Dyn* 2007;236(12):3343-3357.
24. James P, Halladay J, Craig EA. Genomic libraries and a host strain designed for highly efficient two-hybrid selection in yeast. *Genetics* 1996;144(4):1425-1436.
25. Kalchauer I, Farley BM, Pauli S, Ryder SP, Ciosk R. FBF represses the Cip/Kip cell-cycle inhibitor CKI-2 to promote self-renewal of germline stem cells in *C. elegans*. *EMBO J* 2011;30(18):3823-3829.
26. Kedde M, van Kouwenhove M, Zwart W, et al. A Pumilio-induced RNA structure switch in p27-3'UTR controls miR-221 and miR222 accessibility. *Nat Cell Biol* 2010;12(10):1014-1020.
27. Killian DJ and Hubbard EJA. *Caenorhabditis elegans* germline patterning requires coordinated development of the somatic gonadal sheath and the germ line. *Dev Biol* 2005;279(2):322-335.
28. Lee M, Zhao R, Phan L, Yeung SJ. Roles of COP9 Signalosome in Cancer. *Cell Cycle* 2011;10(18):3057-3066.
29. Lin K, Qiang W, Zhu M, et al. Mammalian Pum1 and Pum2 control body size via translational regulation of the cell cycle inhibitor cdkn1b. *Cell Rep* 2019;26(9):2434-2450.
30. Lingaraju GM, Bunker RD, Cavadini S, Hess D, Hassiepen U, Renucci M, Fischer ES, Thomä NH. Crystal structure of the human COP9 signalosome. *Nature* 2014;512(7513):161-5.
31. Meneely PM, Dahlberg CL, Rose JK. Working with worms: *Caenorhabditis elegans* as a model organism. *Current Protocols* 2019;10.1002/cpet.35. Published online September 3, 2019 doi.org/10.1002/cpet.35.
32. Menichelli E, Zu J, Campbell ZT, Wickens M, Williamson JR. Biochemical characterization of *Caenorhabditis elegans* FBF·CPB-1 translational regulation complex identifies conserved protein interaction hotspots. *J Mol Biol* 2013;425(4):725-737.
33. Miles WO, Tschöp K, Herr A, Ji JY, Dyson NJ. Pumilio facilitates miRNA regulation of the E2F3 oncogene. *Genes Dev* 2012;26(4):356-368.

34. Moore FL, Jaruzelska J, Fox MS, et al. Human Pumilio-2 is expressed in embryonic stem cells and germ cells and interacts with DAZ (Deleted in AZoospermia) and DAZ-like proteins. *Proc Natl Acad Sci USA* 2003;100(2):538-543.
35. Morrison SJ, Shah NM, Anderson DJ. Regulatory mechanisms in stem cell biology. *Cell* 1997;88(3):287-298.
36. Naudin C, Hattabi A, Michelet F, et al. PUMILIO/FOXP1 signaling drives expansion of hematopoietic stem/progenitor and leukemia cells. *Blood* 2017;129(18):2493-2506.
37. Orsborn AM, Li W, McEwen TJ. GLH-1, the *C. elegans* P granule protein, is controlled by the JNK KGB-1 and by the COP9 subunit CSN-5. *Development* 2007;134(18):3383-3392.
38. Pazdernik N and Schedl T. Introduction to germ cell development in *Caenorhabditis elegans*. *Adv Exp Med Biol* 2013;757:1-16.
39. Pfaffl MW. A new mathematical model for relative quantification in real-time RT-PCR. *Nucleic Acids Res* 2001;29(9):e45.
40. Qiu C, Bhat VD, Rajeev S, et al. A crystal structure of a collaborative RNA regulatory complex reveals mechanisms to refine target specificity. *Elife* 2019;8:e48968.
41. Schindelin J, Arganda-Carreras I, Frise E, et al. Fiji: an open-source platform for biological-image analysis. *Nat Methods* 2012;9(7):676-682.
42. Schlierf A, Altmann E, Quancard J, et al. Targeted inhibition of the COP9 signalosome for treatment of cancer. *Nat Commun* 2016;7:13166.
43. Sekeres MA, Watts J, Radinoff A, et al. Randomized phase 2 trial of pevonedistat plus azacitidine versus azacitidine for higher-risk MDS/CMML or low-blast AML. *Leukemia* 2021;10.1038/s41375-021-01125-4. Published online January 22, 2021. doi:10.1038/s41375-021-01125-4.
44. Shackelford TJ, Claret FX. JAB1/CSN5: a new player in cell cycle control and cancer. *Cell Dev* 2010;5:26.
45. Sharon M, Mao H, Erba EB, Stephens E, Zheng N, Robinson CV. Symmetrical modularity of the COP9 signalosome complex suggests its multifunctionality. *Structure* 2009;17(1):31-40.
46. Shi P, Zhang J, Li X, Li W, Li H, Fu P. Long non-coding RNA NORAD inhibition upregulates microRNA-323a-3p to suppress tumorigenesis and development of breast cancer through the PUM1/eIF2 axis. *Cell Cycle* 2021;1-13.
47. Shin H, Haupt KA, Kershner AM, Kroll-Conner P, Wickens M, Kimble J. SYGL-1 and LST-1 link niche signaling to PUF RNA repression for stem cell maintenance in *Caenorhabditis elegans*. *PLoS Genet* 2017;13(12):e1007121.
48. Silva ILZ, Robert AW, Cabo GC, et al. Effects of PUMILIO1 and PUMILIO2 knockdown on cardiomyogenic differentiation of human embryonic stem cells culture. *PLoS One* 2020;15(5):e0222373.
49. Smialek MJ, Ilaslan E, Sajek MP, Jaruzelska J. Role of PUM RNA-binding proteins in cancer. *Cancers (Basel)* 2021;13(1):129.
50. Smith P, Leung-Chiu WM, Montgomery R, et al. The GLH proteins, *Caenorhabditis elegans* P granule components, associate with CSN-5 and KGB-1,

- proteins necessary for fertility, and with ZYX-1, a predicted cytoskeleton protein. *Dev Biol* 2002;251(2):333-347.
51. Spassov DS, Jurecic R. Mouse Pum1 and Pum2 genes, members of the Pumilio family of RNA-binding proteins, show differential expression in fetal and adult hematopoietic stem cells and progenitors. *Blood Cells Mol Dis* 2003;20(1):55-69.
 52. Suh N, Crittenden SL, Goldstrohm A, et al. FBF and its dual control of *gld-1* expression in the *Caenorhabditis elegans* germline. *Genetics* 2009;181(4):1249-1260.
 53. Tomoda K, Kato J, Tatsumi E, Takahashi T, Matsuo Y, Yoneda-Kato N. The Jab1/COP9 signalosome subcomplex is a downstream mediator of Bcr-Abl kinase activity and facilitates cell-cycle progression. *Blood* 2005;105(2):775-783.
 54. Voronina E and Greenstein D. Germ cell fate determination in *C. elegans*. In: *eLS* John Wiley & Sons, Ltd;2016:1-8.
 55. Wang H, Huang H, Wang L, et al. Cancer-associated fibroblasts secreted miR-103a-3p suppresses apoptosis and promotes cisplatin resistance in non-small cell lung cancer. *Aging (Albany NY)* 2021;13(10):14456-14468.
 56. Wang X, Ellenbecker M, Hickey B, et al. Antagonistic control of *Caenorhabditis elegans* germline stem cell proliferation and differentiation by PUF proteins FBF-1 and FBF-2. *Elife* 2020;9:e52788.
 57. Wang X, Olson JR, Rasoloson D, Ellenbecker M, Bailey J, Voronina E. Dynein light chain DLC-1 promotes localization and function of the PUF protein FBF-2 in germline progenitor cells. *Development* 2016;143(24):4643-4653.
 58. Wang X, Voronina E. Diverse roles of PUF proteins in germline stem and progenitor cell development in *C. elegans*. *Front Cell Dev Biol* 2020;8:29.
 59. Wei N, Chamovitz DA, Deng XW. Arabidopsis COP9 is a component of a novel signaling complex mediating light control of development. *Cell* 1994;78(1):117-124.
 60. Wei N, Deng XW. COP9: a new genetic locus involved in light-regulated development and gene expression in Arabidopsis. *Plant Cell* 1992;4(12):1507-1518.
 61. Wickens M, Bernstein DS, Kimble J, Parker R. A PUF family portrait: 3'UTR regulation as a way of life. *Trends Genet* 2002;18(3):150-157.
 62. Wolf DA, Zhou C, Wee S. The COP9 signalosome: an assembly and maintenance platform for cullin ubiquitin ligases? *Nat Cell Biol* 2003;5(12):1029-1033.
 63. Yan M, Liu Q. Differentiation therapy: a promising strategy for cancer treatment. *Clin J Cancer* 2016;35:3.
 64. Yoshida A, Yoneda-Kato N, Kato J. CSN5 specifically interacts with CDK2 and controls senescence in a cytoplasmic cyclin E-mediated manner. *Sci Rep* 2013;3:1054.
 65. Zakrzewski W, Dobrzyński M, Szymonowicz M, Rybak Z. Stem cells: past, present, and future. *Stem Cell Res Ther* 2019;10(1):68.
 66. Zarkower D. Somatic sex determination. In *WormBook: The Online Review of C. elegans Biology*, WormBook;2006. Accessed March 15, 2021. <https://www.ncbi.nlm.nih.gov/books/NBK19759/>

67. Zhang B, Gallegos M, Puoti A, et al. A conserved RNA-binding protein that regulates sexual fates in the *C. elegans* hermaphrodite germ line. *Nature* 1997;390(6659):477-484.
68. Zhou L, Jiang Y, Luo Q, Li L, Jia L. Neddylation: a novel modulator of the tumor microenvironment. *Mol Cancer* 2019;18(1):77.